

# Semianalytical approach to short-wavelength dispersion and modal properties of photonic crystal fibers

Niels Asger Mortensen

MIC-Department of Micro and Nanotechnology, Technical University of Denmark, DK-2800 Kongens Lyngby, Denmark

Received January 18, 2005

Photonic crystal fibers made from arbitrary base materials are considered, and a unified semianalytical approach for the dispersion and modal properties is derived that applies to the short-wavelength regime. In particular, the dispersion and the effective index are calculated and compared with fully vectorial plane-wave simulations, and excellent agreement is found. Asymptotic results for the mode-field diameter and the  $V$  parameter are also calculated, and from the latter it is predicted that the fibers are endlessly single mode for a normalized airhole diameter smaller than 0.42, independently of the base material. © 2005 Optical Society of America

OCIS codes: 060.2310, 060.2400, 060.2430.

Photonic crystal fibers (PCFs) are dielectric optical fibers with an array of airholes running along the full length of the fiber. Typically, the fibers employ a single dielectric base material (with dielectric function  $\epsilon_b = n_b^2$ ), and historically silica has been the most common choice.<sup>1,2</sup> Recently other base materials have been studied, including chalcogenide glass, lead silicate glass, telluride glass, bismuth glass, silver halide, teflon, and plastics and (or) polymers. The fabricated fibers typically share the same overall geometry with airholes arranged in a triangular lattice and the core defect being formed by removal of a single airhole. There has been a major theoretical and numerical effort to understand the dispersion and modal properties of silica-based PCFs in particular, but the scale invariance of Maxwell equations<sup>3</sup> cannot be applied directly to generalize the results to other base materials. The reason is that PCFs made from different base materials do not relate to each other by a linear scaling of the dielectric function,  $\epsilon(\mathbf{r}) \rightarrow s^2 \epsilon(\mathbf{r})$ , with  $s$  being a positive scalar. The increased focus on the use of new base materials thus calls for a theory of PCFs with an arbitrary base material.

This Letter offers a unified approach to the dispersion properties that utilizes the fact that the base material typically has a dielectric function exceeding that of air significantly,  $\epsilon_b \gg 1$ . The short-wavelength regime is characterized by having the majority of the electrical field residing in the high-index base material, while the fraction of the electrical field in the airholes is vanishing; see, e.g., Ref. 4. The calculation starts from the fully vectorial wave equation for the electrical field<sup>3</sup>:

$$\nabla \times \nabla \times \mathbf{E}(\mathbf{r}) = \epsilon(\mathbf{r}) \frac{\omega^2}{c^2} \mathbf{E}(\mathbf{r}). \quad (1)$$

For a fiber geometry with  $z$  along the fiber axis we have  $\epsilon(\mathbf{r}) = \epsilon(x, y)$ , and we look for solutions of the plane-wave form  $\exp[i(\beta z - \omega t)]$  with the goal of cal-

culating the dispersion  $\omega(\beta)$  relation. The above discussion for  $\epsilon_b \gg 1$  suggests that we can approximate the problem by imposing the boundary condition that  $\mathbf{E}$  is zero at the interfaces to the airholes. Since the displacement field  $\mathbf{D} = \epsilon \mathbf{E}$  is divergence free we have  $0 = \epsilon \nabla \cdot \mathbf{E} + \mathbf{E} \cdot \nabla \epsilon \approx \epsilon \nabla \cdot \mathbf{E}$ . In the bulk matrix material the latter equality is exact, and the wave equation reduces to

$$-\nabla^2 \mathbf{E}(\mathbf{r}) = \epsilon_b \frac{\omega^2}{c^2} \mathbf{E}(\mathbf{r}), \quad (2)$$

which we solve with the boundary condition that  $\mathbf{E}$  is zero at the interfaces to the airholes. For the boundary condition to be meaningful it is crucial that  $\epsilon_b \gg 1$  so that the fraction of electrical field in the airholes is vanishing in the short-wavelength regime. The wave problem has now become scalar, but it should be emphasized that the approach is very different from the usual scalar treatment<sup>5</sup> and from recent applications to PCFs in the short-wavelength regime<sup>2,4,6</sup> that take the electrical field in the airholes into account. Obviously, the scalar problem posed by Eq. (2) is separable, and formally we have

$$\omega = (\Omega_{xy}^2 + \Omega_z^2)^{1/2} = \frac{c}{n_b} (\gamma^2 \Lambda^{-2} + \beta^2)^{1/2}, \quad (3)$$

where  $\Omega_z = c\beta/n_b$  is the frequency associated with the longitudinal plane-wave propagation,  $\Omega_{xy} = \gamma \times c\Lambda^{-1}/n_b$  is the frequency associated with the transverse confinement and (or) localization, and  $\gamma$  is a corresponding dimensionless and purely geometrical number that depends on only the normalized airhole diameter  $d/\Lambda$ . From Eq. (2) it follows that  $\gamma$  is an eigenvalue governed by a scalar two-dimensional Schrödinger-like equation:

$$-\Lambda^2 (\partial_x^2 + \partial_y^2) \psi(x, y) = \gamma^2 \psi(x, y), \quad (4)$$

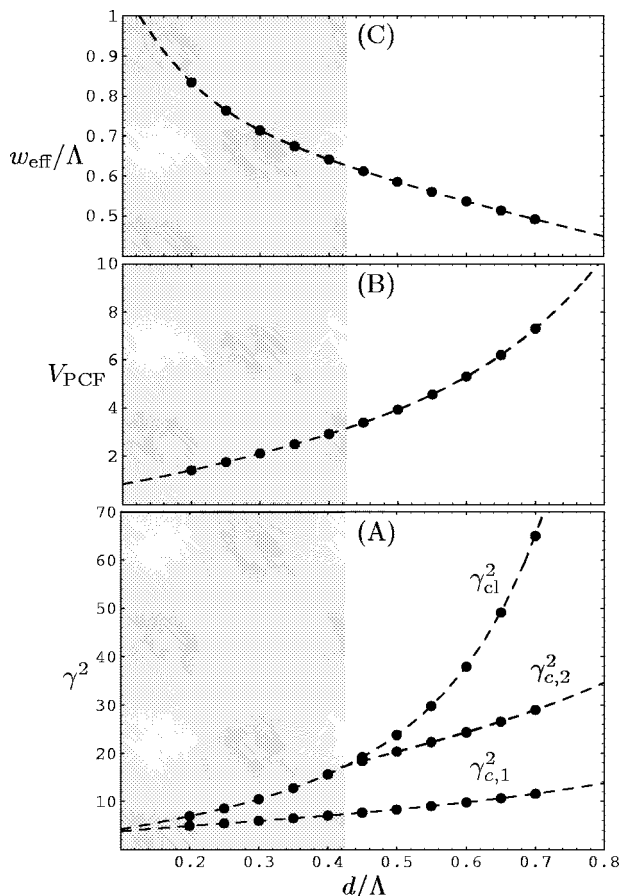


Fig. 1. (A) Geometrical eigenvalues  $\gamma^2$  for the fundamental core (c,1), the second-order core (c,2) and the fundamental cladding (cl) modes versus normalized airhole diameter  $d/\Lambda$ . (B) Corresponding  $V$  parameter. (C) Effective mode-field radius of the fundamental core mode. The data points are obtained from finite-element simulations<sup>7</sup> of Eq. (4), and the dashed curves are guides to the eyes. The gray region indicates the endlessly single-mode regime with  $V_{\text{PCF}} < \pi$ .

with the scalar function  $\psi$  being subject to hard-wall boundary conditions at the interfaces to the airholes, i.e.,  $\psi=0$  in the airholes.

Developments in computational physics and engineering have turned numerical solutions of partial differential equations in the direction of a standard task. Here a finite-element approach<sup>7</sup> is employed to solve Eq. (4) numerically and calculate  $\gamma^2$  versus  $d/\Lambda$ . Figure 1 (A) summarizes the results for the fundamental core mode (see the inset in Fig. 2), the second-order core mode, and the fundamental cladding mode (see the inset in Fig. 3). For the core modes the problem has been truncated by considering a sufficiently large domain with Dirichlet boundary conditions, while for the cladding modes a unit cell with periodic boundary conditions is considered that for symmetry reasons can be formulated in terms of Neumann conditions.<sup>2</sup> As the normalized airhole diameter  $d/\Lambda$  is increased the localization becomes tighter and as expected the eigenvalue increases. For the fundamental core mode the dashed curve shows a third-order polynomial:

$$\gamma_c^2 \approx \mathcal{A} + \mathcal{B} \frac{d}{\Lambda} + \mathcal{C} \left( \frac{d}{\Lambda} \right)^2 + \mathcal{D} \left( \frac{d}{\Lambda} \right)^3, \quad (5)$$

with  $\mathcal{A}=2.67$ ,  $\mathcal{B}=12.51$ ,  $\mathcal{C}=-9.45$ , and  $\mathcal{D}=13.88$  being fitting parameters.

The recently proposed  $V$  parameter,<sup>8</sup>  $V_{\text{PCF}} \equiv \Lambda(\beta_c^2 - \beta_{\text{cl}}^2)^{1/2}$ , becomes

$$\lim_{\lambda \ll \Lambda} V_{\text{PCF}} = (\gamma_{\text{cl}}^2 - \gamma_c^2)^{1/2}, \quad (6)$$

and the numerical results shown in Fig. 1(b) agree nicely with the short-wavelength asymptotic limit of recent simulations of silica-based PCFs.<sup>9</sup> The endlessly single-mode regime<sup>2</sup> defined by  $V_{\text{PCF}} < \pi$  (Ref. 8) exists for  $d/\Lambda \leq 0.42$ , independently of the base material. For more detail on the modal cutoff see Ref. 8 and references therein. Figure 1(c) shows results for the effective mode-field radius<sup>10</sup>  $w_{\text{eff}}$  calculated from  $A_{\text{eff}} \equiv \pi w_{\text{eff}}^2$  with the effective area given by

$$\lim_{\lambda \ll \Lambda} A_{\text{eff}} = \frac{\int dx dy |\psi(x,y)|^2 \int dx' dy' |\psi(x',y')|^2}{\int dx dy |\psi(x,y)|^4}. \quad (7)$$

As expected the mode-field diameter decreases as the normalized airhole diameter is increased, and the mode becomes more localized. For  $V_{\text{PCF}} = \pi$  we find that  $w_{\text{eff}}/\Lambda \approx 0.627$ .

With Eqs. (3) and (5) at hand we now have a unified theory of the dispersion relation in the short-wavelength regime for PCFs with arbitrary base ma-

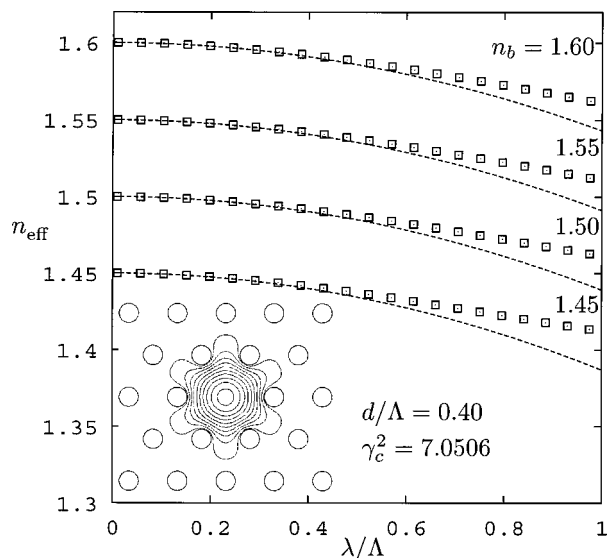


Fig. 2. Effective index  $n_{\text{eff}}$  of the fundamental core mode versus normalized wavelength  $\lambda/\Lambda$  for hole fibers with normalized airhole diameter  $d/\Lambda=0.4$  and varying base material. The dashed curves are the predictions of Eq. (8), and the data points are the results of fully vectorial plane-wave simulations.<sup>11</sup> Inset, fiber geometry and the fundamental core eigenfunction  $\psi_c$  with  $\gamma_c^2=7.0506$ , obtained with a finite-element simulation.<sup>7</sup>

materials, and Eq. (3) illustrates how geometrical confinement modifies the linear free-space dispersion relation.

In fiber optics it is common to express the dispersion properties in terms of the effective index  $n_{\text{eff}} = c\beta/\omega$  versus the free-space wavelength  $\lambda = c2\pi/\omega$ . From Eq. (3) it follows straightforwardly that

$$n_{\text{eff}} = n_b \left[ 1 - \frac{\gamma^2}{4\pi^2 n_b^2} \left( \frac{\lambda}{\Lambda} \right)^2 \right]^{1/2}, \quad (8)$$

which obviously is in qualitative agreement with the accepted view that  $n_{\text{eff}}$  increases monotonically with decreasing wavelength and approaches  $n_b$  in the asymptotic short-wavelength limit as reported for, e.g., silica-based PCFs.<sup>2</sup> However, how good is the quantitative agreement for different base materials? In Figs. 2 and 3 fully vectorial plane-wave simulations<sup>11</sup> are employed to compare Eq. (1) with the predictions of Eq. (8) for the fundamental core

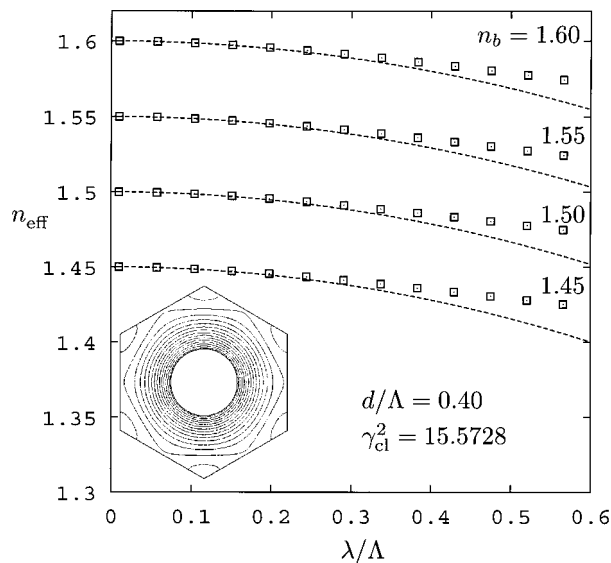


Fig. 3. Effective index  $n_{\text{eff}}$  of the fundamental cladding mode versus normalized wavelength  $\lambda/\Lambda$  for hole fibers with normalized airhole diameter  $d/\Lambda=0.4$  and varying base material. The dashed curves are the predictions of Eq. (8), and the data points are results of fully vectorial plane-wave simulations.<sup>11</sup> Inset, unit cell of the periodic cladding structure and the fundamental cladding eigenfunction  $\psi_{\text{cl}}$  with  $\gamma_{\text{cl}}^2=15.5728$ , obtained with the aid of a finite-element simulation.<sup>7</sup>

and cladding modes, respectively. For the core modes a sufficiently large supercell configuration is employed. As can be seen from the figures, there is an overall good agreement between the fully vectorial numerical results from Eq. (1) and the semianalytical predictions of Eq. (8). In the short-wavelength limit  $\lambda \ll \Lambda$  the agreement is excellent, which underlines the high relevance of the present results to large-mode-area PCFs. As the index of the base material is increased the agreement is even better (results not shown). As the wavelength  $\lambda$  is increased and becomes comparable with the pitch  $\Lambda$  the quantitative agreement is not as good. The reason is well known from small-core silica-based PCFs where a nonnegligible fraction of the electrical field is forced to reside in the airhole regions and where vectorial effects of Eq. (1) also start to matter.

In conclusion, it has been shown how a unified description of the short-wavelength dispersion and modal properties is possible. The theory illustrates how the waveguide dispersion originates from the geometrical transverse localization of the mode, and the semianalytical description of the short-wavelength properties is readily applied to PCFs made from any base material.

This work was supported financially by the Danish Technical Research Council (grant 26-03-0073). N. A. Mortensen's e-mail address is asger@mailaps.org.

## References

1. J. C. Knight, T. A. Birks, P. St. J. Russell, and D. M. Atkin, *Opt. Lett.* **21**, 1547 (1996).
2. T. A. Birks, J. C. Knight, and P. St. J. Russell, *Opt. Lett.* **22**, 961 (1997).
3. J. D. Joannopoulos, R. D. Meade, and J. N. Winn, *Photonic Crystals: Molding the Flow of Light* (Princeton U. Press, Princeton, N.J., 1995).
4. J. Riishede, N. A. Mortensen, and J. Lægsgaard, *J. Opt. A Pure Appl. Opt.* **5**, 534 (2003).
5. A. W. Snyder and J. D. Love, *Optical Waveguide Theory* (Chapman & Hall, New York, 1983).
6. T. A. Birks, D. M. Bird, T. D. Hedley, J. M. Pottage, and P. St. J. Russell, *Opt. Express* **12**, 69 (2004).
7. Femlab, <http://www.comsol.com>.
8. N. A. Mortensen, J. R. Folkenberg, M. D. Nielsen, and K. P. Hansen, *Opt. Lett.* **28**, 1879 (2003).
9. M. D. Nielsen and N. A. Mortensen, *Opt. Express* **11**, 2762 (2003).
10. M. D. Nielsen, N. A. Mortensen, J. R. Folkenberg, and A. Bjarklev, *Opt. Lett.* **28**, 2309 (2003).
11. S. G. Johnson and J. D. Joannopoulos, *Opt. Express* **8**, 173 (2001).